Photodiagnosis and Photodynamic Therapy 29 (2020) 101602

Contents lists available at ScienceDirect

Photodiagnosis and Photodynamic Therapy

journal homepage: www.elsevier.com/locate/pdpdt

Enhanced radiosensitivity of LNCaP prostate cancer cell line by gold-photoactive nanoparticles modified with folic acid

Olya Changizi[a,d], Samideh Khoei[b,c,d,*], Alireza Mahdavian[e], Sakine Shirvalilou[c,d,*], Seied Rabi Mahdavi[d], Jaber Keyvan Rad[e]

[a] Student Research Center, Iran University of Medical Sciences, Tehran, Iran
[b] Razi Drug Research Center, Iran University of Medical Sciences, Tehran, Iran
[c] Finetech in Medicine Research Center, Iran University of Medical Sciences, Tehran, Iran
[d] Department of Medical Physics, School of Medicine, Iran University of Medical Sciences, Tehran, Iran
[e] Polymer Science Department, Iran Polymer & Petrochemical Institute, Tehran, Iran

ARTICLE INFO

Keywords:
Photochromic organic compounds
Folic acid
Cell targeting
Gold nanoparticles
Spiropyran

ABSTRACT

Background: Conventional cancer treatment methods suffer from many limitations such as non-specificity in discrimination between healthy and malignant cells. The aim of this study was to investigate the role of polymeric gold-photoactive nanoparticles (PGPNPs) conjugated with folic acid (FA) as theranostic nanoparticles for active targeting, real-time fluorescence tracing and radiosensitivity inducition in LNCaP prostate cancer cells.
Methods: The cellular uptake and cytotoxicity effect of gold nanoparticles (PGPNPs and PGPNPs-FA) after 2 and 24 h treatment were evaluated in in both cancer (LNCaP) and normal (HUVEC) cells using fluorescent microscopy, Induced coupled plasma optical emission spectrometry (ICP-OES) and Tetrazolium bromide dye (MTT), respectively. The therapeutic efficacy was analyzed on the LNCaP cells. For this purpose, LNCaP cells were treated by nanoparticles and ionizing radiation, and the synergistic effect of treatment methods were evaluated by colony formation assay (CFA) and Flow cytometry analysis.
Results: The results of fluorescence imaging and ICP-OES data showed that the LNCaP cells absorbed PGPNP-FA nanoparticles more than PGPNP ($P < 0.001$). Also, the uptake of nanoparticles was significantly greater in cancer cells than in healthy ones ($P < 0.01$). MTT assay results indicated higher cytotoxic effect of nanoparticles conjugated with FA in folate-receptor overexpressing LNCaP cancer cells compared to HUVEC normal cells ($P < 0.01$). Furthermore, CFA and Flow cytometry results demonstrated that combinatorial therapy of polymeric gold nanoparticles with/without FA and ionizing radiation at various doses (2, 4 and 6 Gy) had a synergistic effect on survival fraction and induction of apoptotic and necrotizing cell death ($P < 0.01$).
Conclusion: PGPNPs-FA nanoparticles led to higher and more specific uptake and accumulation of nanoparticles in LNCaP cells, thereby increasing the ability of gold nanoparticles as radio-sensitizer.

1. Introduction

Prostate cancer (PCa) is the second common reason of death among men around the world, which kills about 250,000 patients a year [1]. Surgery, chemotherapy and radiotherapy are commonly used methods to treat this type of cancer. Non-specificity and the potential for severe damage to healthy tissue is one of the most important problems in routine treatments [2]. Generally, more than 50 % of patients are treated with radiation therapy, which has limitations in achieving high dose to the tumor area and the protection of the healthy tissue surrounding the tumor. There are two main strategies to these challenges: the use of radio screensavers or the use of radio sensors [3]. Recently, new technologies have developed to overcome such limitations where nanotechnology role seems the most important [4]. Nanomaterials became variously applied in clinic due to physical, chemical, optical and size related properties such as high surface/volume ratio and biocompatibility [5]. Recent advances in nanotechnology has introduced smart nanomaterials, applicable in active targeting approach. By modifying the surface of nanoparticles with ligands whose receptors are specifically over-expressed on the surface of the cancer cells, the anticancer agents can be transmitted specifically to the tumor cells, which is known as active targeting [6,7]. Targeted nanomaterial selectively

* Corresponding authors at: Razi Drug Research Center, Finetech in Medicine Research Center, Department of Medical Physics, School of Medicine, Iran University of Medical Sciences, P.O. Box: 1449614525, Tehran, Iran.
E-mail addresses: khoei.s@iums.ac.ir, skhoei@gmail.com (S. Khoei), shirvaliloo.s@tak.iums.ac.ir, sakine.shirvaliloo@gmail.com (S. Shirvalilou).

https://doi.org/10.1016/j.pdpdt.2019.101602
Received 6 June 2019; Received in revised form 24 October 2019; Accepted 12 November 2019
Available online 14 November 2019
1572-1000/

binds to and affects cancer cells which made their application more advantageous to compare with other treatment methods [8]. Folic acid, an essential vitamin, has critical role in cell proliferation. Cellular membrane of special cancer cell lines including head and neck, breast, ovary, uterus and prostate express abundant folic acid receptors [9]. So that combining folic acid with other therapeutic materials can facilitate effective targeting of cancer cells [10]. Among targeting methods based on physical and biological differences between healthy and cancer cells, this method is used efficiently [11]. In dynamic targeting, in order to increase the access of particles to desired tissue, a mixture of bound ligands to particle surface with high affinity to distinct molecules is used. Specific binding can facilitate ligand dependent endocytosed to internalize particles into the cells [12]. Folate (acid folic salt) is one of the required components in purine and pyrimidine biosynthesis in DNA replication process [13]. Rapid cell division in cancer cells leads to higher demand of folate and hence cancer cells express more folate receptors [14]. Folate properties such as stability, easy combination, lack of immune system simulation, higher specific receptor affinity ($Kd \approx 10^{-9}$) and rapid penetration to cancer cells made it suitable element for targeting approach [14,15]. Recently, the use of gold nanoparticles modified with folic acid has been considered as an effective factor in targeted radiation therapy. But it will be even more interesting to use nanoparticles for tracking, sensing or labeling [16].

Gold Nanoparticle (GNPs) is one of the best options in cancer treatment since it is biocompatible, easy to synthesis, chemo-physical stable and own adjustable optical properties [17]. Recently, gold nanoparticle was introduced as radio-sensitizers [18]. Both the physical and the biological aspects are important to understand the radiosensitivity of the gold nanoparticles. In addition to the high atomic number, the radius of a sensitizer agent also directly affects radiotherapy yield by effecting on photoelectric cross-section collision [19]. Based on this physical reality, ionizing radiation intensely absorbs by gold nanoparticles possessing high atomic number (Z = 79). GNPs also show a high radiation sensitivity due to a greater atomic radius than gold atom (~0.17 nm) [20]. In addition to sensitizing radiation properties of gold nanoparticles, it has recently reported that bound folate to gold nanoparticles can be applied as an effective agent in targeting radiotherapy [21]. Gold nanoparticles bound to folic acid thorough receptor dependent endocytosis, enters those cells that express folic acid receptor on their cell surface. Moreover, the internalization, in order to achieve efficient therapy beside targeted one; nanoparticles aggregation inside cancer cells has to increase specifically. For this purpose, binding to biological molecules like folate is possible [16].

Fluorescent microscopy is an efficient tool in live cell and tissue imaging, which unlike other techniques, is capable of dynamic imaging of live cell processes. Spiropyran derivatives are the most suitable photochromic organic compounds [22]. Fisher discovered Photochromic properties of Spiropyran in 1952 [23]. These characteristics are present in soluble phase. Spiropyran molecule in closed form is nonpolar and consists of two perpendicular halves. Thus, less pairing happens between these halves, it remains colorless and called Spiro (SP) form. The carbon-oxygen bond breaks upon UV radiation [24]. Thus, in Spiropyran derivatives, radiation cause reversible break in CO bond opens colorless, non-polar ring of SP and turns it to Merocynanin (MC) isomer that is in contrast, colorful and polar. So, SP is used as fixed colorful Merocynanin in polymer form for optical imaging [25]. In this paper, we attempted to study the role of polymeric gold nanoparticles as fluorescent carrier in homocysteine bed for tracing and radio-sensitizing according to acid folic and gold nanoparticles effects. Here, the influence of presence and absence of acid folic was studied on prostate cancer cells (LNCaP) in comparison with healthy cells (HUVEC). Considering applied fluorescence nature of the nanoparticle, the nanoparticle presence can be analyzed by optical imaging in every stage.

2. Material and methods

2.1. Material

All materials, reagents and solvents for synthesis of nanoparticles were supplied by Merck and Sigma-Aldrich (Germany) except for 2,2-Azobis [2-(2- imidazoline-2-yl) propane] dihydrochloride (VA-044), that was obtained from Wako Pure Chemical Industries Ltd (Osaka, Japan). LNCaP and HUVEC cell lines derived from the human prostate adenocarcinoma was purchased from the cell bank of the Pasteur Institute of Iran. Cell culture medium (RPMI), Fetal bovine serum (FBS) and Penicillin-Streptomycin were purchased from Atocel (Austria).

2.2. Synthesis of folic acid conjugated polymer coated gold photoresponsive nanocomposites (PGPNPs-FA)

The synthesis of polymeric gold nanoparticles was carried out in three steps:

2.2.1. Preparation of photo responsive latexes containing Spiropyran and Imidazole (PNPsIm)

Preparation of Spiropyran photochromic compound was performed according to the previously reported procedure [22]. Semi-continuous emulsion polymerization method was used to prepare polymeric nanoparticles containing photochromic compound in the inner parts and n-vinyl imidazole monomer in the outer part. For this purpose, 70 ml of aqueous solution of cetyl trimethyl ammonium bromide as a cationic stabilizer (CTAB, 300 mg), and 60 mg of VA-044 initiator were prepared and transferred to the three-necked round bottom reactor. Then, 20 ml of Spiropyran acid ethyl acrylate monomers (SPEA, 200 mg) solution and 5.7 ml of methyl methacrylate monomer (MMA) were added to the reaction vessel. Next, the mixture of monomers of MMA (1.5 mL) and N-vinyl imidazole (NVIM, 0.2 mL) were added to the reaction vessel dropwise.

2.2.2. Preparation of the polymer-gold photoresponsive nanocomposites (PGPNPs)

After preparation of functionalized latexes containing Spiropyran and Vinyl imidazole, the chloride Au^{3+} ions were deposited on the surface of polymeric nanoparticles (PNPsIm) using in situ reduction method. For this purpose, 65 ml of $HAuCl_4.3H_2O$ (3 g/L) was added to 35 ml of the prepared latex (prepared previous step) and stirred for 24 h. Then, 23 ml of sodium borohydride (3 g/L) were added dropwise and the stirrer continued for 1 h. At last, as the reaction progressed, the color of the mixture changed from yellow to violet [21].

2.2.3. Preparation of the polymer-gold photoresponsive nanocomposites functionalized with folic acid (PGPNPs-FA)

The L-cysteine was used for conjugation of the folic acid compound to the surface of gold nanoparticles as an intermediate. Initially, the mixture of folic acid (250 mg, 0.57 mmol) and 4-(dimethylamino) pyridine (DMAP) (18 mg, 0.15 mmol) were added to anhydrous dimethyl sulfoxide (DMSO) and stirred at room temperature for one hour. N, N′-dicyclohexylcarbodiimide (DCC) (118 mg, 0.57 mmol) was then dissolved in 10 ml of dichloromethane (DCM) and solution was added to the reaction mixture. After one hour, 69 mg L-cystine (0.57 mmol) in DCM (10 ml) was added dropwise to the reaction vessel, the stirrer continued for 24 h. Then, DCM (100 mL) was added to the above solution, centrifuged and the reaction precipitate was isolated. After, 150 mg of the obtained product (FA-Lcys) was dissolved in distilled water (20 ml), and the ammonia solution was added to the reaction solution to neutralize pH. The obtained solution was added dropwise into the 30 ml of the previously prepared latex containing polymer-gold photo responsive nanocomposites (PGPNPs) and the mixture was stirred for overnight. Finally, after purifying the PGPNPs-FA with a dialysis bag, the nanoparticles were dried via freeze-drying.

2.3. Characterization of nanoparticles

Dynamic light scattering analysis was used to characterize the distribution of the hydrodynamic size and diameter of nanoparticles (PGPNPs and PGPNPs-FA). Also, the surface charge of nanoparticles was investigated by Zeta sizer (Nanoflex, Germany). The morphological investigation of the both nanoparticles was obtained using a Transmission electron microscope (TEM, Zeiss LEO906, Germany). The samples were prepared on 400-mesh carbon coated copper grid.

2.4. Biological experiments

2.4.1. Cell culture procedure

LNCaP human prostate cancer cells and HUVEC human umbilical vein endothelial cells were cultured in a complete RPMI and Ham's F-12 medium supplemented with 10 % FBS, penicillin (100 U/mL) and streptomycin (100 mg/mL) at a concentration of 10,000 cells/cm^2 within humidified incubator with 5 % carbon dioxide at 37 ˚C, respectively.

2.4.2. Cellular uptake of Nanoparticles (PGPNPs and PGPNPs-FA)

Targeted transfer efficiency of nanoparticles in LNCaP cells with high expression of folate receptors and HUVEC cells with low expression were investigated by two methods. A) qualitative method by fluorescence microscopy and B) quantitative method by induced coupled plasma spectroscopy.

2.4.2.1. Fluorescence microscopy. The confirmation of the entry of nanoparticles into the LNCaP and HUVEC cells and tracing them in two groups of nanoparticles with and without folic acid ligand was performed at different incubation times 2 and 24 h. The cells were seeded in 6-well plates at a density of 100000 cells/well in 1.5 ml of complete RPMI and Ham's F-12 medium. After 24 h, the medium was removed and cells incubated with 0.01 mg/ml of PGPNPs with/without FA ligand for 2 h and 24 h. Then, the medium was removed and the wells were washed twice with PBS. Cells were fixed with 2 % formaldehyde for 30 min. Fluorescence images of the cells were taken with a fluorescence microscope (Olympus CK2; Olympus Optical Co., Tokyo, Japan). The wells are subjected to an excitation wavelength (365 nm), and the emission wavelength of the sample was $550-560$ nm.

2.4.2.2. Induced coupled plasma optical emission spectrometry (ICP-OES). Two million LNCAP and HUVEC cells per wells were seeded. After 24 h, the cells were treated with gold nanoparticles with/without folic acid ligand for two times, 2 and 24 h. Then, the medium was removed and the cells were harvested after 3 times washing with PBS. Then, aqua regia solution (1–3 ratio of HNO_3 65 % and HCl 37 %) was added to samples at 140 ˚C for 1 h to digest all the nanoparticles and cellular content. The amount of gold in the samples was determined by ICP-OES assay (VISTAPRO, Varian, Australia).

2.5. In vitro cytotoxicity assay

The toxicity of the gold nanoparticles with and without folic acid ligand was evaluated by the MTT cell viability assay. The LNCAP and HUVEC cells were seeded in a 96-well microplate at a density of 8000 cells/well in 100 µl of complete medium. After 24 h, the cells were treated with different concentrations ($0-10$ mg/ml) of nanoparticles (PGPNPs, PGPNPs-FA) for 2 and 24 h. Then, the MTT solution was prepared (5 mg/mL) in PBS. Wells washed twice with PBS for removal of the nanoparticles. Then, 100 µl of the MTT solution was added to each well and plates were incubated in incubator for 4 h. After, the MTT solution was discharged and 200 µl of dimethyl sulfoxide (DMSO) was added to each well. The plate was then incubated for $15-20$ min and the absorbance (570 nm-test/630 nm-reference) was read by an ELIZA reader. Finally, concentration via viability curves were obtained and the half maximal inhibitory concentration (IC50) values were calculated.

2.6. Treatment with ionizing radiation

The irradiation of LNCaP cell line was performed using 6 MV X-ray photons with different doses (2, 4 and 6 Gy) at the Asia Hospital. The radiation procedure was performed by a linear accelerator (Siemens, Germany). To achieve the dosage of 4 and 6 Gys, the irradiation of the cells with the dose of 2 was repeated two and three times. The flasks were completely filled with complete RPMI culture medium (in order to ensure the uniformity of radiation to the cells). The flasks were arranged side by side and irradiated with these conditions: Field dimensions was 20×20 cm, the distance from the radiation source to the bottom of the flask (Source surface distance) was 100 cm, the monitor unit was 193 and the Gantry angle was 180 degrees.

2.7. In vitro antitumor efficacy of nanoparticles

2.7.1. Colony formation assay (CFA)

Colony formation assay was performed to evaluate the colony formation ability of the LNCaP cells after treatments. For this purpose, 24 h after incubation, the cells were treated with (0.01 mg/ml) of nanoparticles (PGPNPs, PGPNPs-FA) only or combined with ionizing radiation (2, 4 and 6 Gy), the cells were cultured in different concentrations, and according to the doubling time of the cells, counting the colonies were carried out after eight days. The colonies were fixed with formaldehyde 2 % and stained with Crystal Violet color for 20 min. The efficiency of cell therapy was evaluated by calculating the plating efficiency (PE) by the following equation 1:

$$\text{Plating efficiency } (\%) = (\text{Number of obtained colonies}/\text{Number of seeded cells}) \times 100 \quad (1)$$

And the surviving fraction (SF) is also obtained by the following equation:

$$\text{Surviving fraction} = (\text{Plating efficiency of treated cells}/\text{Plating efficiency of control cells}) \times 100 \quad (2)$$

2.7.2. Cell apoptosis assay

Flow cytometry was used to determine the apoptotic death rate of LNCaP cells induced by PGPNPs, PGPNPs-FA (0.01 mg/ml) and ionizing radiation (2, 4 and 6 Gy), alone or in combination. After treatment, the cells were harvested and trypsinized. Then, 1 ml of 1X binding buffer was added to cells (treated and untreated) and it was resuspended. Next, 5 µl of Annexin FITC was added to each sample and incubated for 15 min in dark conditions, at room temperature. Then 5 µl of Propidium iodide (PI) was added and following that, the absorbance of the samples was analyzed by a flow cytometer (BD, San Jose, USA).

2.8. Statistical analysis

All tests were repeated at least three times, and the results were expressed as mean ± standard deviation (SD). For statistical analysis of data, GraphPad Prism 6 was used. One-way ANOVA followed by Tukey's test were used to compare the groups. A value of $P < 0.05$ was considered to be statistically significant.

3. Results

3.1. Characterization of nanoparticles

The average size of gold nanoparticles alone was about 12 nm, and when added to the polymer, the average size of PGPNPs is about 47 nm.

Table 1
Size and zeta potential of PGPNPs with and without FA ligand. (n = 3, mean ± SD).

Nanoparticles	Particle size (nm)	PDI	ζ potential (mV)
PGPNPs	46.2 ± 0.92	0.16	−31.63 ± 0.02
PGPNPs-FA	55.09 ± 0.06	0.2	−28.85 ± 0.18

The results of the size distribution and surface charge of PGPNPs and PGPNPs-FA nanoparticles are shown in Table 1. PGPNPs nanoparticles had a size of 46.2 ± 0.92 nm and a Zeta potential of -31.63 ± 0.02 mV, which was 55.9 ± 0.06 nm and -28.85 ± 0.18 mV for PGPNPs-FA nanoparticles, respectively. Adding folic acid ligand increased the size of the nanoparticles and decreased the absolute magnitude of the zeta potential. Spherical morphology, uniform distribution, and size of nanoparticles based on TEM images are shown in Fig. 1. The dark and light regions showed regions pointed by blue and red arrows are related to Gold nanoparticles and polymer substrate, respectively. The size of the nanoparticles obtained from the TEM images was lower than that of the DLS analysis, which is due to the type of preparation of samples used in two methods, in the TEM method, a dry sample and in DLS method dissolved samples in aqueous phase are used.

3.2. Confirmation of the entrance of nanoparticles to the cells

Targeted entrance of nanoparticles into the LNCaP and HUVEC cells based on the fluorescence properties of nanoparticles were shown in Fig. 2, qualitatively. According to the obtained images, the control group of cells that have not uptake any nanoparticles lack fluorescence radiation and the images were dark; on the contrary, the cells that have uptake nanoparticles with folic acid exhibited the highest fluorescence radiation (especially after 24 h of incubation). However, the results showed that the rate of fluorescence was significantly higher in LNCaP cells due to the higher expression of folic acid receptors at the cell surface than in HUVEC cells ($P < 0.001$). Furthermore, the amount of entered nanoparticles to the cells was measured by the amount of Au^{3+} ions in pictograms per cell, using ICP-OES (Fig. 3). The amount of nanoparticle uptake for two PGPNPs and FA-PGPNPs nanoparticles after 2 h incubation treatment based on Pg/cell was 0.02 ± 0.001 and 0.023 ± 0.001 Pg/cell, for HUVEC and 0.019 ± 0.002 and 0.041 ± 0.003 Pg/cell, for LNCaP cells respectively. The amount of nanoparticle uptake for two PGPNPs and FA-PGPNPs nanoparticles after 24 h incubation treatment based on Pg/cell was 0.081 ± 0.003 and 0.095 ± 0.001 Pg/cell, for HUVEC and 0.087 ± 0.002 and 0.25 ± 0.011 Pg/cell, for LNCaP cells respectively. As shown, the entrance of FA-PGPNPs nanoparticles after 24 -h treatment was significantly higher than that of PGPNPs in both cells ($P < 0.05$). However, according to fluorescence imaging data (Fig. 2), the uptake of FA-conjugated nanoparticles was significantly increased in LNCaP cancer cells, which was 2.63-fold higher than in normal HUVEC cells ($P < 0.001$). However, no similar effect was observed for PGPNPs without folic acid ligand (Fig. 3). In addition, the nanoparticle entrance was time-dependent and higher entrance was detected after 24 h incubation compared to 2 h incubation.

3.3. Toxicity evaluation of PGPNP and FA-PGPNP nanoparticles on LNCaP cells

The toxicity of PGPNP and FA-PGPNP nanoparticles on LNCaP and HUVEC cells after 2 and 24 h of incubation was assessed by the MTT cell viability assay. According to the results shown in Fig. 4, representing the percentage of live cells at the different concentrations of the nanoparticle, the toxicity increases with increasing nanoparticle concentration as well as the duration of treatment. Comparing the results of MTT assay for the treated cells with different types of nanoparticles showed that the gold nanoparticles conjugated with folic acid are more toxic than gold nanoparticles without any conjugation ($P < 0.05$, Fig. 4A & C). In addition, the IC50 values (the concentration of nanoparticles, which cause 50 % death of cells) for both nanoparticles with different incubation times (2 and 24 h) were calculated

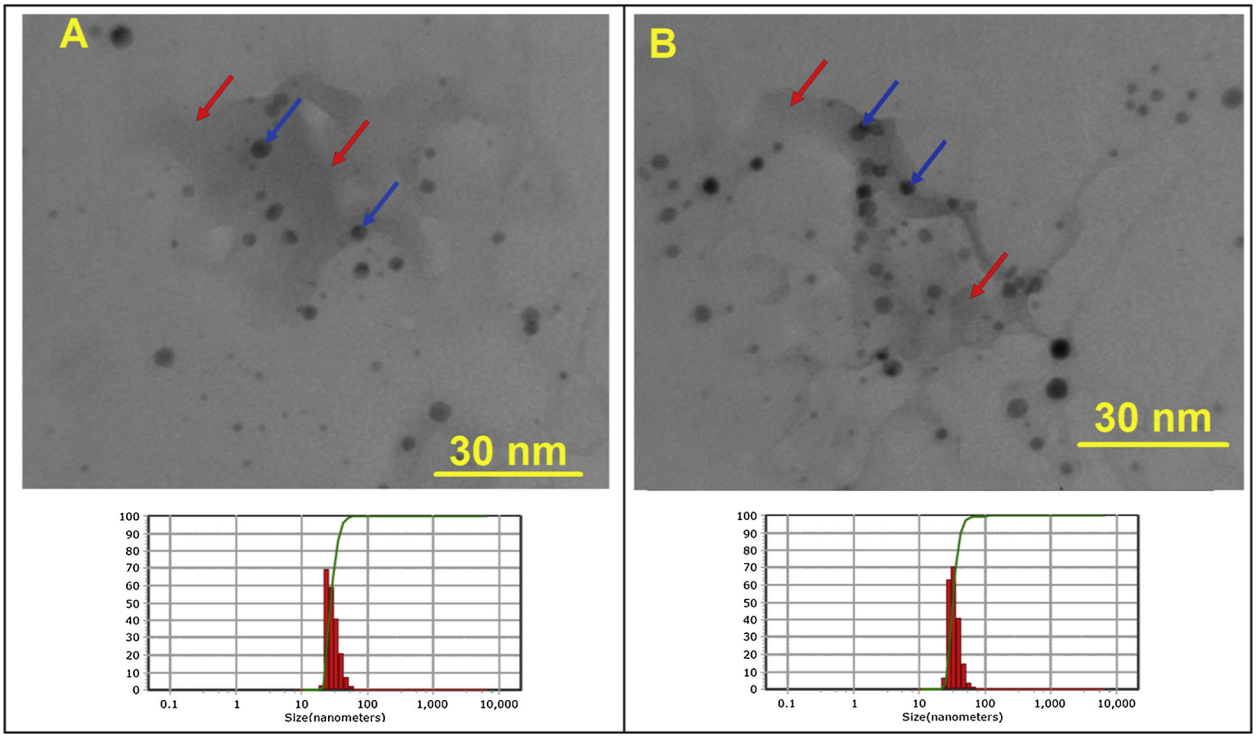

Fig. 1. TEM image and size distribution; A) Gold nanoparticles (PGPNPs). B) Gold nanoparticles modified with folic acid (PGPNPs-FA). The blue and red arrows indicate the dark and light regions, that are related to Gold nanoparticles and polymer substrate, respectively.

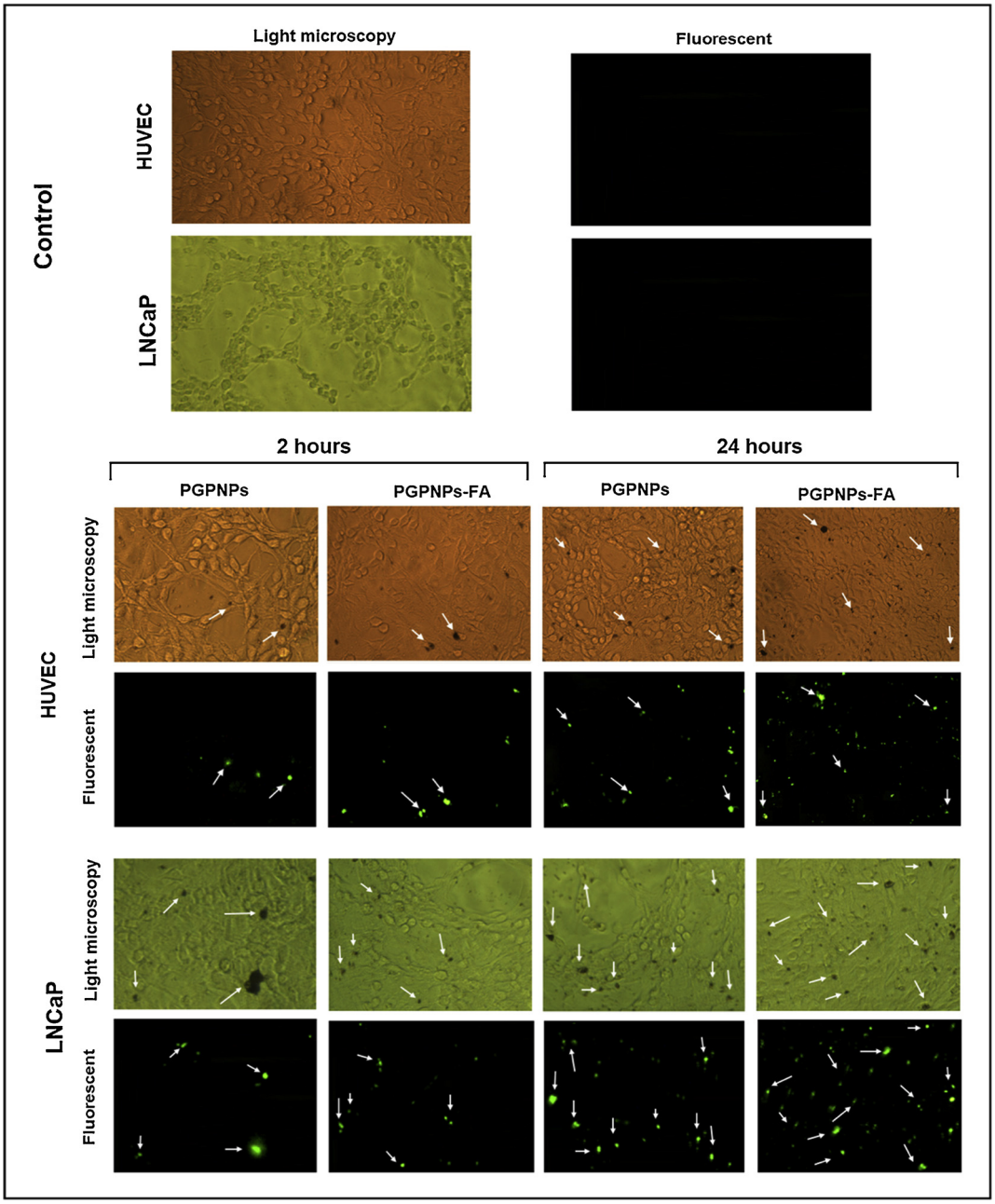

Fig. 2. The nanoparticle uptake by LNCaP cells and HUVEC cells, using a fluorescence microscopy, the images related to the visible light and the images related to fluorescence microscope are shown for control cells, PGPNP nanoparticles after 2 and 24 h' incubation, and PGPNP-FA nanoparticles after 2 and 24 h' incubation.

according to Fig. 4A & C. As shown in Fig. 4B, the IC50 values after 2 h treatment of PGPNPs and PGPNPs-FA nanoparticles were equal to 0.358 ± 0.012, and 0.326 ± 0.021 mg/ml for HUVEC cells and 0.427 ± 0.026, and 0.334 ± 0.017 mg/ml for LNCaP cells, respectively (Fig. 4B). It was found that there was no significant difference among the cytotoxicity of PGPNPs and PGPNPs-FA in HUVEC cells ($P > 0.05$), whereas the toxicity was significant in LNCaP cells ($P < 0.05$). The IC50 values after 24 h treatment of PGPNPs and PGPNPs-FA nanoparticles decreased to 0.24 ± 0.01, and 0.205 ± 0.004 mg/ml for HUVEC cells and 0.28 ± 0.011, and 0.135 ± 0.006 mg/ml for LNCaP cells, respectively (Fig. 4D). After 24 h treatment, the cytotoxic effect of PGPNPs-FA was significantly higher than that of PGPNPs in LNCaP cells ($P < 0.001$) but there was no significant difference between two type of nanoparticles in HUVEC cells ($P > 0.05$), which indicated a remarkable potential for PGPNPs-FA nanoparticles in targeting tumors.

3.4. Determination of the effect of PGPNG and FA-PGPNG nanoparticles or their ionized radiation on LNCaP cells

The results of colony formation assay showed no significant difference in colonogenic death of cells of LNCaP between treated cells with radiation (2 h and 24 h after treatment) compared to the control group ($P > 0.05$, Fig. 5). However, colony formation assay showed that the rate of colonogenic death increased by increasing ionized radiation dosages (Fig. 5). These results were in accordance with the results of flow cytometry test. According to the flow cytometry results, PGPNP or 2 Gy radiation did not induce any significant cell death when applied alone ($P > 0.05$, Figs. 6 and 7).

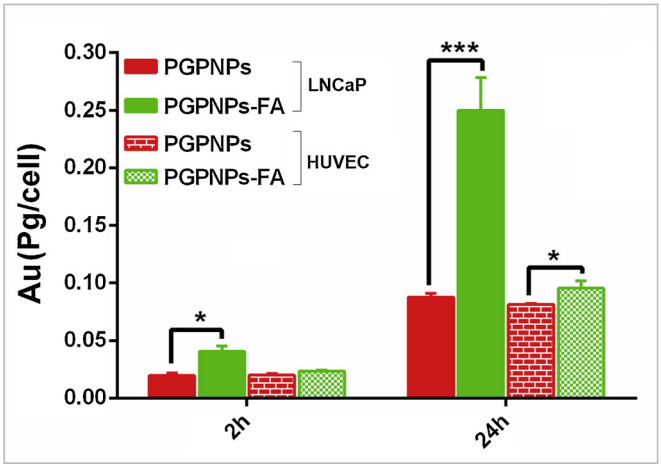

Fig. 3. The amount of Au absorbed by LNCaP and HUVEC cells, 2 and 24 h after treatment, using ICP-OES analysis, (Mean ± SD, n = 3, statistical significance was showed with (*) P < 0.05, (**) P < 0.01 and (***) for P < 0.001, respectively).

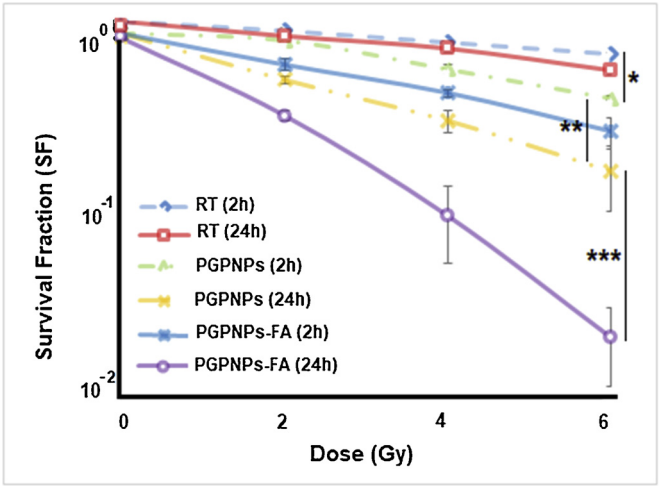

Fig. 5. The survival fraction of LNCaP cells after combinational therapy (PGPNPs and PGPNPs-FA only or combined with radiation 2, 4 or 6 Gy) in different groups. (Mean ± SD, n = 3, statistical significance was showed with (*) P < 0.05, (**) P < 0.01 and (***) for P < 0.001, respectively).

3.5. Determination of the effects of PGPNG and FA-PGPNG nanoparticles in combination with ionized radiation on LNCaP cells

Colony formation assay showed that the combined effect of radiation and nanoparticles with/without FA during 2 h and 24 h after radiotherapy significantly reduced cell survival fraction (P < 0.01, Fig. 5). Also, according to the flow cytometry results, there was significant difference in the amount of induced apoptosis by different doses of ionized radiation in different time after radiation (P < 0.05). The percentage of apoptosis deaths induced using PGPNPs and PGPNP-FA nanoparticles in combination with different ionized radiation ranges in both 2-h and 24-h after treatments were significantly increased compared to the only ionized radiation in all three dosages of 2, 4 and 6 Gys (P < 0.05, Figs. 6 and 7). In addition, the percentage of cell death was considerably increased by the use of PGPNP-FA nanoparticles compared to the use of PGPNP nanoparticles (P < 0.05). Finally, the results colony formation assay (Fig. 5) and Flowcytometry (Figs. 6 and 7) indicate increased cell death in the combination of nanoparticles (PGPNP and PGPNP-FA) and radiation, which could represent a significant potential for gold nanoparticles to improve radiotherapy efficacy.

4. Discussion

Since the early 1960s, radiotherapy has been used as the main treatment for advanced prostate cancer [26]. Although radiation dose increases can kill cells, early and late side effects often limit the use of

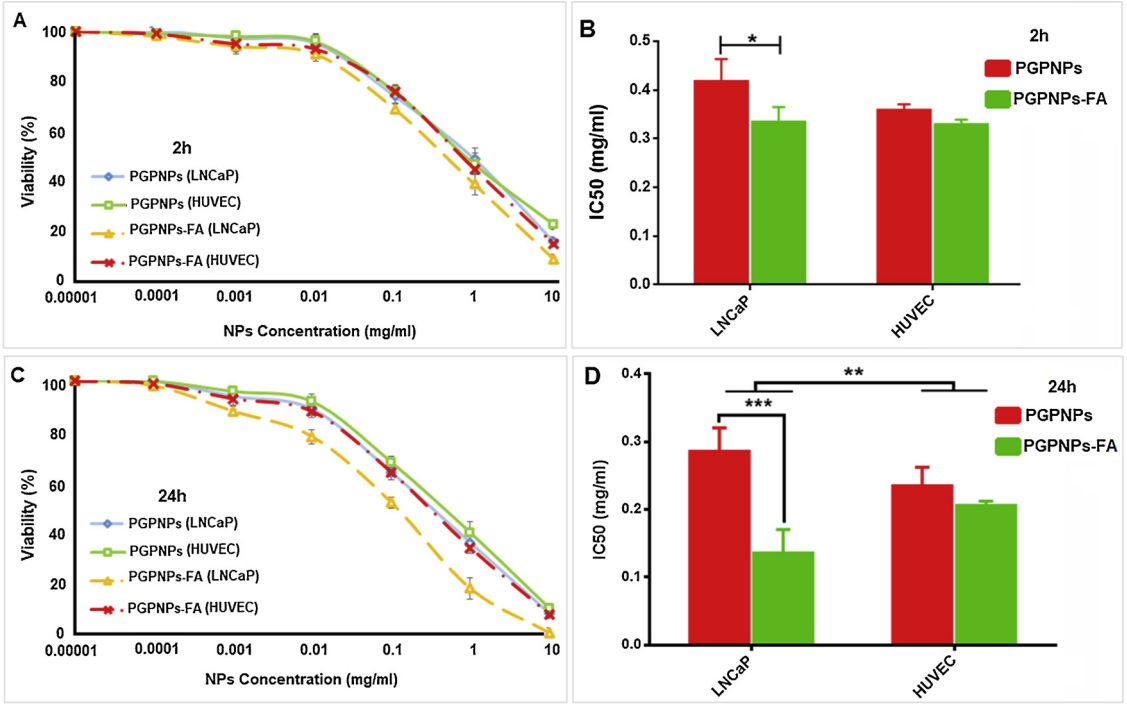

Fig. 4. Cytotoxic effects of LNCaP and HUVEC cells treated with different concentrations of PGPNPs and PGPNPs-FA nanoparticles, A) 2 h and C) 24 h incubation. The IC50 values of PGPNPs and PGPNPs-FA, B) after 2 and, D) 24 h of treatment. (Mean ± SD, n = 3, statistical significance was showed with (*) P < 0.05, (**) P < 0.01 and (***) for P < 0.001, respectively).

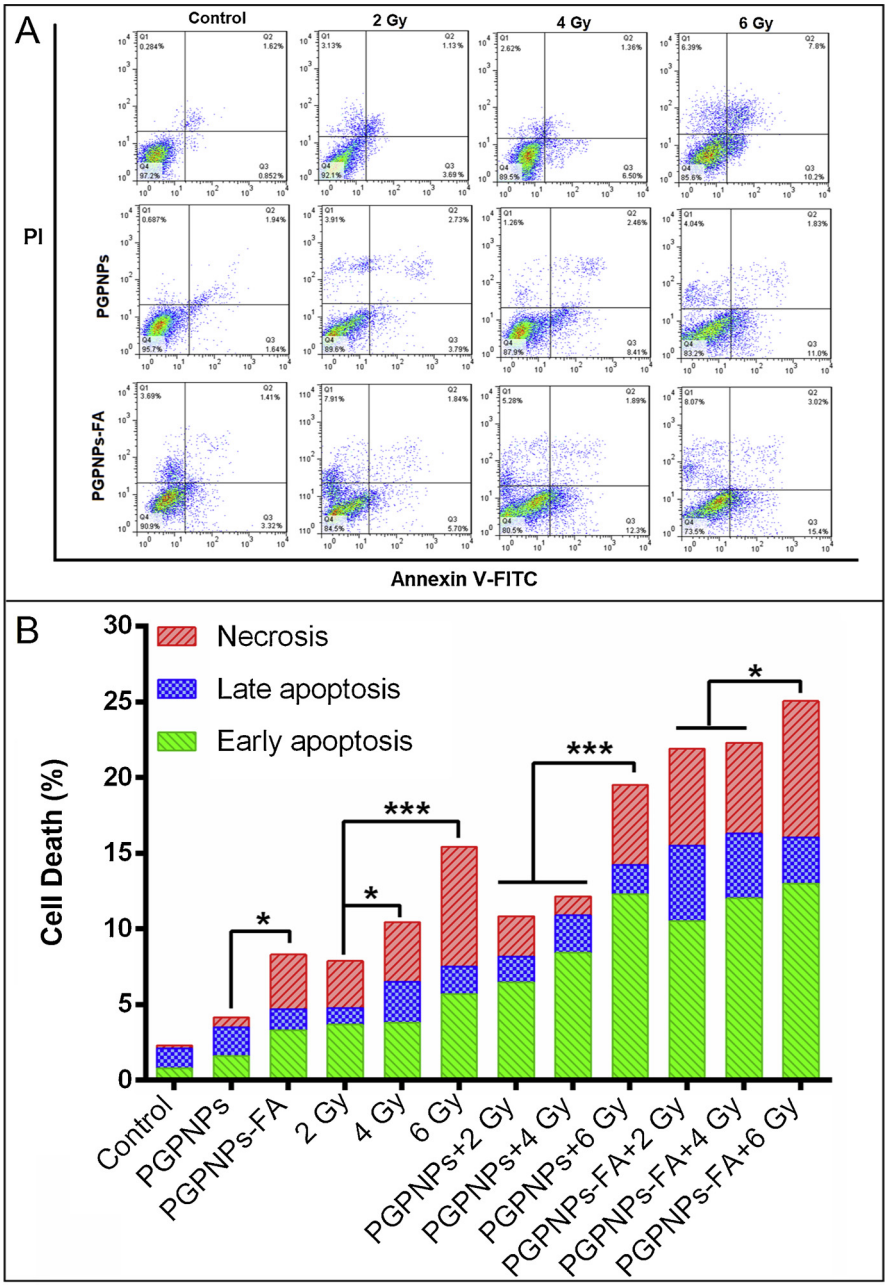

Fig. 6. A) The Annexin-V/PI staining assay for detecting the apoptosis of LNCaP cells. B) The percentage of apoptosis and necrotic cells, 2 h after treatment with PGPNPs and PGPNPs-FA only or combined with radiation 2, 4 or 6 Gy. (Mean ± SD, n = 3, statistical significance was showed with (*) $P < 0.05$, (**) $P < 0.01$ and (***) for $P < 0.001$, respectively).

high radiation doses. Therefore, recent research is aimed at increasing therapeutic efficacy in low doses of radiation [27]. Accordingly, in this study the synergistic effect of radiosensitive gold nanoparticles mediated with FA ligand was studied with the aim of enhancing the radiation therapy efficacy in LNCaP prostate cancer cells.

In confirmation of past studies, our results showed that radiotherapy of LNCaP prostate cancer cells using photonic energy of 6 MV in different dosages increased clonogenic death immediately after treatment, but has no significantly effect on apoptosis ($P > 0.05$). Bromfield et al. (2003), has also evaluated ionizing radiations on apoptotic checkpoint and cell cycle to analyze the main death mode in different prostate cancer cell lines (LNCaP, DU145 and PC-3). Their results illustrated that apoptosis induction due to ionizing radiation was minimal (6 %) after radiation with dosage of 10 Gy. They have shown that apoptotic cell death is not significantly related with clonogenic death and apoptosis is not the main death mode caused by ionizing radiation [28]. Also, Ha et al. has analyzed the expression of 84 effective genes in different apoptosis pathways in LNCaP and PC-3 cell lines. The results showed no significant changes in apoptosis induction after 10 Gy x-ray radiation for both cell lines [29].

As explained in section 1, gold nanoparticles have a high potential radiosensitizing, but this depends on different parameters, including the size of the nanoparticles, cell uptaking, and the position of the nanoparticles in the cell relative to the nucleus [30,31]. Cho et al. (2009) and Ngwa et al. (2011) have argued that the accumulation of gold nanoparticles of less than 100 nm in tumor cells, especially near the cell nucleus, would increase cell death [32,33].

Therefore, in the first step, using fluorescence images and ICP-OES data (Figs. 2 and 3), we proved that both synthesized nanoparticles (PGPNP and PGPNP-FA) with a size less than 60 nm (Fig. 1) can enter

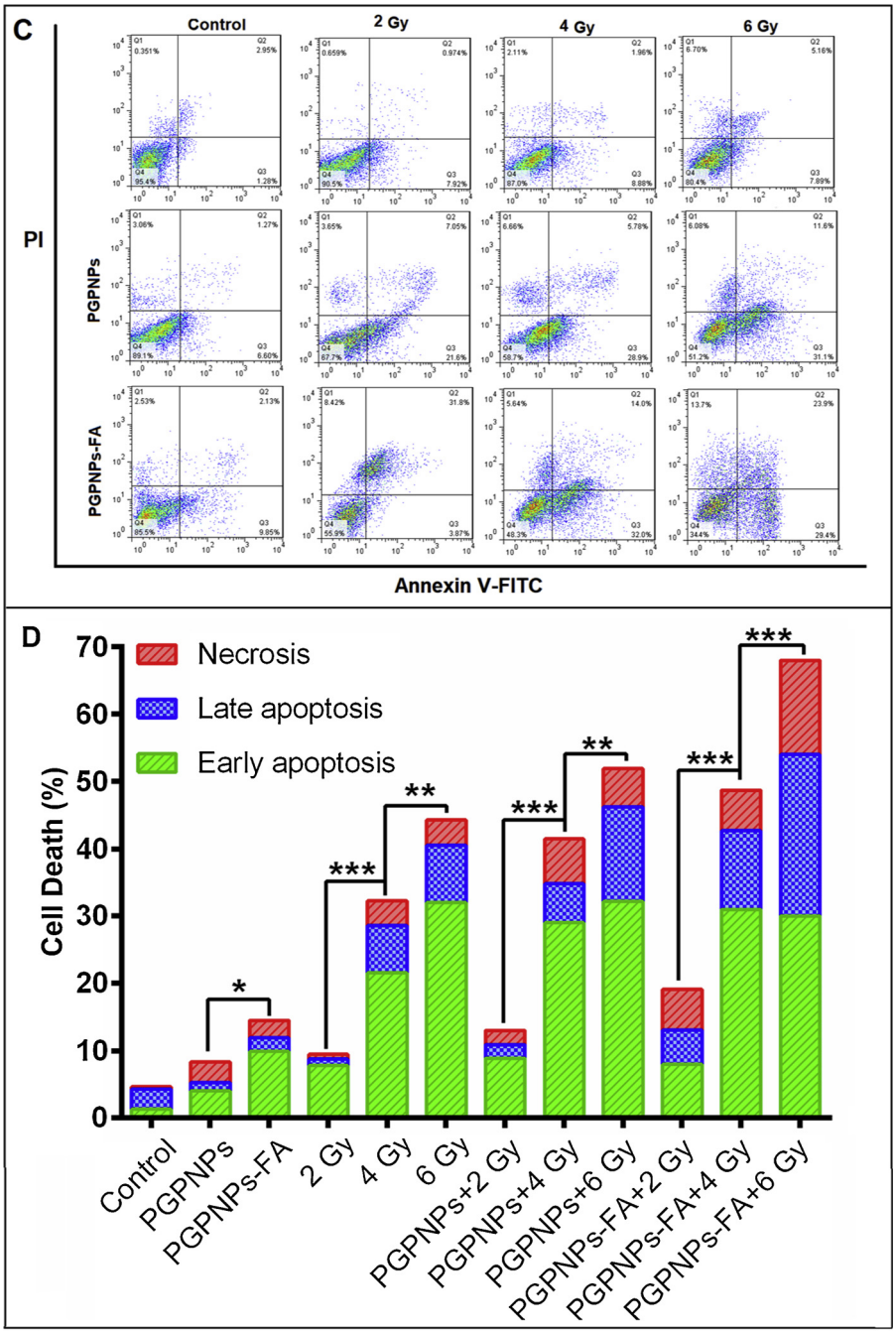

Fig. 7. A) The Annexin-V/PI staining assay for detecting the apoptosis of LNCaP cells. B) The percentage of apoptosis and necrotic cells, 24 h after treatment with PGPNPs and PGPNPs-FA only or combined with radiation 2, 4 or 6 Gy. (Mean ± SD, n = 3, statistical significance was showed with (*) $P < 0.05$, (**) $P < 0.01$ and (***) for $P < 0.001$, respectively).

the LNCaP and HUVEC cells. However, as expected, the uptake rate due to the Folic acid ligand was significantly higher for PGPNP conjugated with FA in LNCaP cells ($P < 0.01$, Figs. 2 and 3). In addition, the results showed that PGPNP-FA nanoparticles were highly targeted to LNCaP cancer cells compared to normal HUVEC cells.

Toxicity assay of nanoparticles showed that nanoparticles can decrease cell viability as well as cell growth trend. However, enhanced cytotoxicity effect was obtained for FA-conjugated nanoparticles in LNCaP cells compared to HUVEC cells ($P < 0.001$). This could be attributed to the enhanced internalization of targeted PGPNP-FA by the cancer cells, due to over-expression of folate-receptor on the surface of cancer cells [34].

In the next step, the effects of combination therapy of radiation and nanoparticles with/without FA on LNCaP cells were investigated, which showed that gold nanoparticle application as radiosensitizer in LNCaP cell line has increased clonogenic as well as apoptotic death in a dosage dependent manner (Figs. 5–7). The presence of gold metal atoms with high atomic number inside cells leads to secondary electrons production due to radiation interaction to compare with particle absence [35]. Numerous studies have proved gold nanoparticles radio-sensitizing property [36,37]. The disagreements between results of different studies can be caused by difference in concentration of gold nanoparticles, type of nanoparticle coating as well as cell lines. However, few studies were conducted in the field of sensitizing these nanoparticles in mega voltage. Jain et al. (2011) has also used gold nanoparticles with glucose coat (GLU-GNPs) as radio-sensitizer to improve radiotherapy in SK-OV-

3 ovary cells and the amount of reactive oxygen species was analyzed by confocal microscopy [37]. They have evaluated induced apoptosis via flow cytometry as well. Their results indicated that growth inhibition has increased 35.48 % and 26.88 % respectively in 90KVp and 6 MV group using nanoparticles to compare with radiation alone. This investigation has also showed that ionizing radiation with gold nanoparticles increased ROS production. Author stated that the effect of gold nanoparticles on apoptosis amount in mega voltage energy is not caused due to high atomic number of gold solely. Albeit gold nanoparticles can cause such effect through changing cell cycle and ceasing cell in radio-sensitive phase of G_2/M. In addition, ROS production increase while radiation interaction with gold nanoparticles, is the main mechanism of apoptosis induction in cancer cell [38]. In our study, acid folic was used for cancer cell targeting as well as more specific treatment and the results showed the effect of acid folic on clonogenic and apoptotic cell death increase [39]. One the intrinsic characteristics of some cancer cells is high expression of acid folic receptor in cell membrane. Acid folic molecules can enter cells via protein carriers and foliate reduced carriers apart from acid folic receptor endocytosis. Huang et al. has prepared transonic particle (treatment-diagnose) consist of gold nanotube as core, silica as stabilizer and folate as targeting agent. The have conducted studies to evaluate radio-sensitizing ability in cancer cells using gold nanoparticles-silica bounded folate. The MGC803 cell gastric cancer was radiated by 6 MV X-ray and cell viability has gradually decreased with nanoparticles bounded folate [3]. Therefore, the results of this paper were in agreement with previous results.

5. Conclusion

In this study, gold nanoparticles were used as a radio-sensitizer as well as folic acid as targeting agent. Besides, due to the fluorescence properties of the nanoparticles, their detection and tracing was conducted by fluorescence microscopy. The results showed that gold nanoparticles in mega -voltage energies and dosages of 2–6 grays could exhibit radio-sensitizing effects. The use of folic acid as a targeting agent was successful.

Declaration of Competing Interest

The authors report no conflicts of interest. The authors alone are responsible for the content and writing of the paper.

Acknowledgement

This research was supported by Razi Drug Research Center, Iran University of Medical Sciences (IUMS) (Grant No. 30236).

References

[1] R.L. Siegel, K.D. Miller, A. Jemal, Cancer statistics, 2015, CA Cancer J. Clin. 65 (1) (2015) 5–29.
[2] B.B.S. Cerqueira, et al., Nanoparticle therapeutics: technologies and methods for overcoming cancer, Eur. J. Pharm. Biopharm. 97 (2015) 140–151.
[3] P. Huang, et al., Folic acid-conjugated silica-modified gold nanorods for X-ray/CT imaging-guided dual-mode radiation and photo-thermal therapy, Biomaterials 32 (36) (2011) 9796–9809.
[4] D.J. Bharali, S.A. Mousa, Emerging nanomedicines for early cancer detection and improved treatment: current perspective and future promise, Pharmacol. Ther. 128 (2) (2010) 324–335.
[5] H. Ghaznavi, et al., Association study of methylenetetrahydrofolate reductase C677T mutation with cerebral venous thrombosis in an Iranian population, Blood Coagul. Fibrinolysis 26 (8) (2015) 869–873.
[6] Y. Patil, et al., Targeting of folate-conjugated liposomes with co-entrapped drugs to prostate cancer cells via prostate-specific membrane antigen (PSMA), Nanomed. Nanotechnol. Biol. Med. 14 (4) (2018) 1407–1416.
[7] K. Rahme, J. Guo, J.D. Holmes, Bioconjugated gold nanoparticles enhance siRNA delivery in prostate cancer cells, RNA Interference and Cancer Therapy, Springer, 2019, pp. 291–301.
[8] R. Bazak, et al., Cancer active targeting by nanoparticles: a comprehensive review of literature, J. Cancer Res. Clin. Oncol. 141 (5) (2015) 769–784.
[9] H. Samadian, et al., Folate-conjugated gold nanoparticle as a new nanoplatform for targeted cancer therapy, J. Cancer Res. Clin. Oncol. 142 (11) (2016) 2217–2229.
[10] J. Sudimack, R.J. Lee, Targeted drug delivery via the folate receptor, Adv. Drug Deliv. Rev. 41 (2) (2000) 147–162.
[11] S. Iyer, et al., Atomic force microscopy detects differences in the surface brush of normal and cancerous cells, Nat. Nanotechnol. 4 (6) (2009) 389.
[12] I. Brigger, C. Dubernet, P. Couvreur, Nanoparticles in cancer therapy and diagnosis, Adv. Drug Deliv. Rev. 64 (2012) 24–36.
[13] J.D. Byrne, T. Betancourt, L. Brannon-Peppas, Active targeting schemes for nanoparticle systems in cancer therapeutics, Adv. Drug Deliv. Rev. 60 (15) (2008) 1615–1626.
[14] B. Yu, et al., Receptor-targeted nanocarriers for therapeutic delivery to cancer, Mol. Membr. Biol. 27 (7) (2010) 286–298.
[15] M.S. Soltanpour, et al., Methylenetetrahydrofolate reductase C677T mutation and risk of retinal vein thrombosis, J. Res. Med. Sci. 18 (6) (2013) 487.
[16] K. Khoshgard, et al., Radiosensitization effect of folate-conjugated gold nanoparticles on HeLa cancer cells under orthovoltage superficial radiotherapy techniques, Phys. Med. Biol. 59 (9) (2014) 2249.
[17] W. Cai, et al., Applications of gold nanoparticles in cancer nanotechnology, Nanotechnol. Sci. Appl. 1 (2008) 17.
[18] J.F. Hainfeld, et al., Radiotherapy enhancement with gold nanoparticles, J. Pharm. Pharmacol. 60 (8) (2008) 977–985.
[19] S. Kargar, et al., Evaluation of the combined effect of NIR laser and ionizing radiation on cellular damages induced by IUdR-loaded PLGA-coated nano-graphene oxide, Photodiagnosis Photodyn. Ther. 21 (2018) 91–97.
[20] X.-D. Zhang, et al., Size-dependent radiosensitization of PEG-coated gold nanoparticles for cancer radiation therapy, Biomaterials 33 (27) (2012) 6408–6419.
[21] J. Keyvan Rad, et al., Enhanced photogeneration of reactive oxygen species and targeted photothermal therapy of C6 glioma brain cancer cells by folate-conjugated gold-photoactive polymer nanoparticles, ACS Appl. Mater. Interfaces (2018).
[22] J. Keyvan Rad, et al., FRET phenomenon in photoreversible dual-color fluorescent polymeric nanoparticles based on azocarbazole/spiropyran derivatives, Macromolecules 49 (1) (2015) 141–152.
[23] Y. Hirshberg, E. Fischer, Multiple reversible color changes initiated by irradiation at low temperature, J. Chem. Phys. 21 (9) (1953) 1619–1620.
[24] R. Klajn, Spiropyran-based dynamic materials, Chem. Soc. Rev. 43 (1) (2014) 148–184.
[25] W. Wu, A.D. Li, Optically Switchable Nanoparticles for Biological Imaging, (2007).
[26] P.L. Nguyen, A.L. Zietman, High-dose external beam radiation for localized prostate cancer: current status and future challenges, Cancer J. 13 (5) (2007) 295–301.
[27] X. Zhang, et al., Enhanced radiation sensitivity in prostate cancer by gold-nanoparticles, Clin. Invest. Med. 31 (3) (2008) 160–167.
[28] G. Bromfield, et al., Cell death in irradiated prostate epithelial cells: role of apoptotic and clonogenic cell kill, Prostate Cancer Prostatic Dis. 6 (1) (2003) 73.
[29] Z. He, et al., Expression profile of apoptosis related genes and radio-sensitivity of prostate cancer cells, J. Radiat. Res. 52 (6) (2011) 743–751.
[30] K.P. Steckiewicz, et al., Impact of gold nanoparticles shape on their cytotoxicity against human osteoblast and osteosarcoma in in vitro model. Evaluation of the safety of use and anti-cancer potential, J. Mater. Sci. Mater. Med. 30 (2) (2019) 22.
[31] D.T. Savage, J.Z. Hilt, T.D. Dziubla, In vitro methods for assessing nanoparticle toxicity, Nanotoxicity, Springer, 2019, pp. 1–29.
[32] S.H. Cho, B.L. Jones, S. Krishnan, The dosimetric feasibility of gold nanoparticle-aided radiation therapy (GNRT) via brachytherapy using low-energy gamma-/x-ray sources, Phys. Med. Biol. 54 (16) (2009) 4889.
[33] W. Ngwa, G.M. Makrigiorgos, R.I. Berbeco, Gold nanoparticle-aided brachytherapy with vascular dose painting: estimation of dose enhancement to the tumor endothelial cell nucleus, Med. Phys. 39 (1) (2012) 392–398.
[34] S.E. Minaei, et al., In vitro anti-cancer efficacy of multi-functionalized magnetite nanoparticles combining alternating magnetic hyperthermia in glioblastoma cancer cells, Mater. Sci. Eng. C 101 (2019) 575–587.
[35] W.N. Rahman, et al., Enhancement of radiation effects by gold nanoparticles for superficial radiation therapy, Nanomed. Nanotechnol. Biol. Med. 5 (2) (2009) 136–142.
[36] A. Saberi, et al., Gold nanoparticles in combination with megavoltage radiation energy increased radiosensitization and apoptosis in colon cancer HT-29 cells, Int. J. Radiat. Biol. 93 (3) (2017) 315–323.
[37] S. Jain, et al., Cell-specific radiosensitization by gold nanoparticles at megavoltage radiation energies, Int. J. Radiat. Oncol. Biol. Phys. 79 (2) (2011) 531–539.
[38] F. Geng, et al., Thio-glucose bound gold nanoparticles enhance radio-cytotoxic targeting of ovarian cancer, Nanotechnology 22 (28) (2011) 285101.
[39] A. Garcia-Bennett, M. Nees, B. Fadeel, In search of the holy grail: folate-targeted nanoparticles for cancer therapy, Biochem. Pharmacol. 81 (8) (2011) 976–984.